geosciences

MDPI

Article

Compositional Diversity of Early Mesozoic Granites in South Qinling: Derivation from Heterogenous Basement Rocks in the Orogenic Belt

Risheng Ye [1], Weiyong Li [1], Dongyang Huo [1], Jingxin Zhao [1], Xiguang Huang [2,*], Jun He [1,*] and Fukun Chen [1]

[1] School of Earth and Space Sciences, University of Science and Technology of China, Hefei 230026, China; lajolla@mail.ustc.edu.cn (R.Y.); weiyongli@mail.ustc.edu.cn (W.L.); huodongyang@mail.ustc.edu.cn (D.H.); zhaojx2020@mail.ustc.edu.cn (J.Z.); fkchen@ustc.edu.cn (F.C.)

[2] Key Laboratory of Green and High-End Utilization of Salt Lake Resources, Qinghai Institute of Salt Lakes, Chinese Academy of Sciences, Xining 810008, China

* Correspondence: xiguanghuang@mail.ustc.edu.cn (X.H.); jhe1989@ustc.edu.cn (J.H.)

Abstract: Granitic rocks forming in the syn- to post-orogenic stages can trace the compositional and structural complexity of the crust beneath an orogenic belt. The Qinling orogenic belt undertook multiple stages of tectonics and magmatism, resulting in the multifaceted evolution and compositional diversity of the crust. In the present study, the Guangtoushan and Miba plutons in South Qinling were chosen to reveal the crustal heterogeneity in study area via isotopic geochemistry and zircon geochronology. The Guangtoushan pluton was emplaced between ~215 Ma and ~202 Ma and the Miba pluton formed at ~213 Ma, as constrained by zircon U-Pb isotopic dating. Granitic rocks of the Miba pluton are characterized by amphibole bearing and homogeneous composition, with relatively depleted Sr-Nd isotopic compositions (initial $^{87}Sr/^{86}Sr$ values of 0.7060 to 0.7084 and initial ε_{Nd} values of −5.4 to −9.5) and high Pb isotopic values. The Guangtoushan pluton contains muscovite and complex inherited zircon grains and has variable Sr-Nd isotopic composition (initial $^{87}Sr/^{86}Sr$ values of 0.7050 to 0.7091 and initial ε_{Nd} values of −4.5 to −12.9) and low Pb isotopic values. Felsic magmas of the Guangtoushan pluton should be derived mainly from meta-sedimentary rocks beneath South Qinling, while the Miba pluton originated primarily from partial melting of meta-igneous rocks. The compositional diversity recorded in the Early Mesozoic plutons was caused by the heterogeneous crust, and partial melting was induced by heating of the up-welling asthenosphere in a post-collision setting.

Keywords: Qinling orogenic belt; Early Mesozoic; granite; compositional diversity; Sr-Nd-Pb isotopes; isotopic age; inherited zircon; magma source

Citation: Ye, R.; Li, W.; Huo, D.; Zhao, J.; Huang, X.; He, J.; Chen, F. Compositional Diversity of Early Mesozoic Granites in South Qinling: Derivation from Heterogenous Basement Rocks in the Orogenic Belt. *Geosciences* **2024**, *14*, 138. https://doi.org/10.3390/geosciences14050138

Academic Editors: Jesus Martinez-Frias and José Manuel Castro

Received: 9 April 2024
Revised: 15 May 2024
Accepted: 16 May 2024
Published: 18 May 2024

1. Introduction

As is commonly known, the origin of compositional diversity in intermediate to felsic igneous rocks is one of the most important questions in the field of petrology. Chemical features of granitic magmas are controlled largely by constituents of source rocks and conditions of partial melting and can be severely modified by petrologic processes, e.g., magma mixing and mingling, assimilation, and fractional crystallization during the magma transfer [1–3]. Previous experiments have shown that compared to the melts produced by partial melting of metapelitic rocks, those originating from partial melting of metamorphosed mafic rocks, have high $CaO/(MgO + {}^{T}FeO)$ as well as low K_2O/Na_2O and $Al_2O_3/(MgO + {}^{T}FeO)$ values, and the meta-greywacke source yields the melts falling the middle range of pelite and mafic rocks [3]. Earlier studies have also confirmed that the chemical composition of the melt depends not only on the components of source rocks, but is also controlled by the conditions of partial melting [2]. Systematical study of compositional diversity in granitic rocks can help us better understand the generation and evolution of continental crust.

Late Triassic granitic magmatism extensively developed in the Qinling orogenic belt and the products can provide ideal objects for us to comprehend the diversity of granodioritic rocks. Based on several previous studies, numerous large granitoid plutons of Early Mesozoic age are exposed in the South Qinling terrain; they consist of complex rock types and were formed in different tectonic settings in the late orogenic stages that resulted from the final collision between the South and North China blocks. They are characterized by compositional variances in elemental and isotopic compositions [4–6], but the origin of this compositional diversity still needs to be further comprehended. In the present study, the Guangtoushan and Miba granitoid plutons, exposed adjacent to the Hui-Cheng basin, were selected as concrete objects. Integrating the previous results in the literature with zircon U-Pb isotopic geochronology and whole-rock elemental and Sr-Nd-Pb isotopic geochemistry of these two plutons, the compositional diversity among different granitoid plutons and different rocks of an individual pluton and the origin concerning the magma source and magmatic process are discussed.

2. Geological Setting

The Qinling orogenic belt in central China is usually subdivided into four tectonic units, from north to south, including the southern margin of the North China block, North Qinling, South Qinling, and northern margin of the Yangtze block, separated by three major fault zones [7–9] (Figure 1a). This orogenic belt has been interpreted to be generated by multiple stages of the continental collision and finally converged in Early Mesozoic between the North and South China blocks [7–12].

The South Qinling terrain, being the major frame of the orogenic belt, is bounded by the Paleozoic Shang-Dan suture zone in north and the Early Mesozoic Mian-Lue suture zone in south (Figure 1a). Many rock units, such as the Archean Yudongzi and Paleoproterozoic Douling groups, which represent the ancient basement, are exposed in this terrain [13–15]. They are mainly composed of amphibolite, felsic gneiss, schist, and marble, occurring as tectonic slices. The Wudang and Yaolinghe groups, characterized by Neoproterozoic volcanic–sedimentary series, usually suffer from a low-grade metamorphic overprint [16,17]. Neoproterozoic and Silurian to Devonian intermediate to felsic intrusive rocks were found mostly in the eastern part of South Qinling [18,19]. The basement of South Qinling is covered mainly by the Devonian to Carboniferous sedimentary sequences and partly by the Permian to Triassic sandstone [9].

Late Triassic granitic rocks are mostly widespread in South Qinling but less widespread in North Qinling (Figure 1a) and are proposed to have been formed in the tectonic setting of the assembly of the South China (or Yangtze) block and South Qinling [20–22]. They are exposed as large plutons usually in the terrain, constituting intermediate to felsic rocks in composition, and are often emplaced in different time or magmatic stages, ranging from ~250 Ma to ~180 Ma [20–24]. Representatives of these are the Miba, Guangtoushan, Wulong, and Dongjiangkou plutons in the east of the Hui-Cheng basin [6,25,26] and the Baoji and Mishuling plutons in the north of the basin [5,27]. Several plutons contain numerous mafic microgranular enclaves, such as the Miba, Dongjiangkou, and Mishuling plutons [5,6], and have geochemical characteristics of I-type granite, while some large plutons, e.g., the Guangtoushan and Baijiazhuang plutons, have an S-type affinity in geochemical composition and mineral assemblage [4,26]. These Triassic rocks in South Qinling have wide variations in geochemical composition and mineral assemblage, implying diversely magmatic origins, such as the Miba, Guangtoushan, Mishuling, and Wulong plutons [4–6,26,27]. These granitic rocks were magmatic products derived from diversely tectonic settings, commonly interpreted as subduction-related [28], early subduction-related to late continental collision [12,24,27,29,30], or syn- to post-collisional settings [31] in the literature. The diversity in the origin and geochemical composition of these rocks is principally caused by their tectonic settings and emplacement ages relative to the final collision time of the Yangtze block and South Qingling.

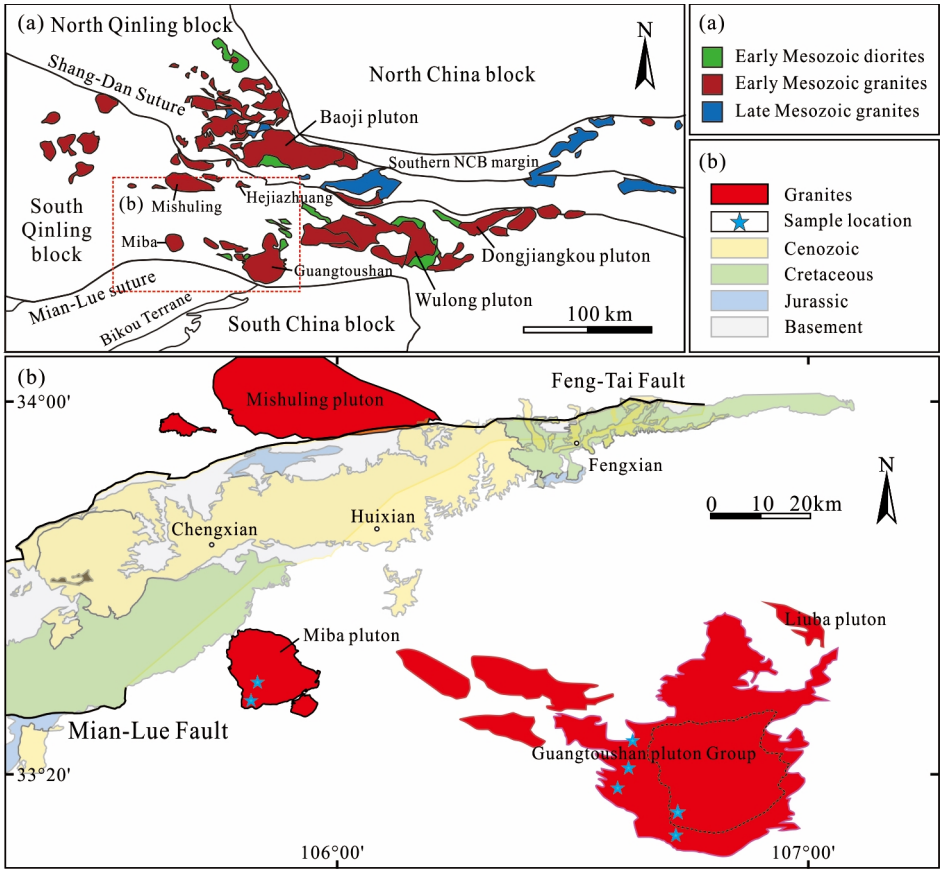

Figure 1. (**a**) Sketched map of the middle part of the Qinling orogenic belt showing the distribution of Mesozoic granite plutons and (**b**) Early Mesozoic granite plutons adjacent to the Hui-Cheng basin [32].

3. Analytical Methods

Major element contents of whole-rock powders, obtained by grinding fresh rock samples to 200 mesh, were measured by using a PANalytical AXIOS X-ray fluorescence (XRF) spectrometer at Australian Laboratory Services (ALS) in Guangzhou, China. Loss on ignition (LOI) was determined by the gravimetric analysis by weighing 1 g sample powder and heating it to 1100 °C for one hour. Analytical uncertainties of major elements were better than 1%. Trace element contents were measured using a Perkin-Elmer ELAN 6100 DRC II ICP-MS at the University of Science and Technology of China (USTC). Analytical results of the United States Geological Survey (USGS) reference rock powders AGV-2 and BHVO-2 suggested the relative deviation of the accuracy was better than 5% for most elements and ~10% for Rb, Zr, and Hf elements. Detailed analytical procedure is available elsewhere [33].

Zircon grains, separated from rock samples via the standard procedure, were hand-picked under a binocular microscope and then mounted in epoxy resin. The grains were polished to expose the cores for the measurements of cathodoluminescence (CL) images and U-Pb isotopic ages. Zircon U-Pb isotopic dating was performed by using a laser-ablation inductively coupled plasma mass spectrometry (LA-ICP-MS) at the USTC. For the ablation, diameter of the laser pit was 32 μm and laser frequency was 10 Hz. Reference materials NIST SRM 610 and 612 and standard zircon 91500 were used for external calibration, and ^{29}Si (32.7% SiO_2 in zircon) was used as an internal standard to calculate concentrations and ages. Details of the analytical technique and process are available elsewhere [34]. Age calculation and concordia plotting were performed by using the ISOPLOT software package [35].

An amount of ~100 mg of whole-rock powder was completely decomposed in a mixture solution of purified HF-HNO_3-$HClO_4$ acid for the Sr-Nd isotopic analysis and in a mixture solution of purified HF-HNO_3 acid for the Pb isotopic analysis. Sr and REEs were separated on a quartz column with the AG50W-X12 (200–400 mesh) ion exchange resin, while Nd was separated from other REEs via the LN ion exchange resin. Pb was separated on a Teflon® column containing ~80 µL AG1-X8 (100–200 mesh) ion exchange resin and employing the HBr-HCl acid wash and elution procedure. Procedural blanks were <200 pg for Sr and <100 pg for Pb and Nd. Isotopic ratios were measured on a ThermoFisher Triton Plus thermal ionization mass spectrometer in the Laboratory for Radiogenic Isotope Geochemistry at USTC. The repeated analyses of NIST SRM 987 Sr and La Jolla Nd solution gave weighted mean values of 0.710241 ± 0.000012 (2σ) and 0.511869 ± 0.000006 (2σ), respectively. A reference solution of Pb (NBS SRM 981) was repeatedly measured for the mass fractionation of Pb isotopic ratios. The analytical techniques were given elsewhere [36].

4. Petrologic Features of the Guangtoushan and Miba Plutons

The Guangtoushan pluton, with an exposure area of about 900 km^2 and sitting on the north of the Mian-Lue suture zone, belongs to the major body of the Guangtoushan pluton group (Figure 1b). According to field observations, granites of this pluton intruded into the strongly deformed Devonian sedimentary sequences within the suture zone in the south and into the low-grade metamorphosed Silurian sedimentary rock in the north [37]. Based on petrologic and geochemical evidence, this pluton was subdivided into internal and marginal phases [32,38]; the internal phase consists mainly of fine- to medium-grained porphyritic monzogranite and two-mica granite, while the marginal phase is mainly composed of fine-grained monzogranite and granodiorite. In the present study, eight monzogranite, three granite, and two granodiorite samples were collected from this pluton. Photographs of representative rock samples in field and under microscope are shown in Figure 2. The major mineral assemblages of monzogranite are ~35% plagioclase, ~35% K-feldspar (perthite), ~25% quartz, and ~5% biotite and muscovite. Granite is composed of ~20% plagioclase, ~45% K-feldspar (perthite), ~30% quartz, and ~5% biotite and muscovite, while granodiorite contains ~55% plagioclase, ~20% K-feldspar (perthite), ~20% quartz, and ~5% biotite.

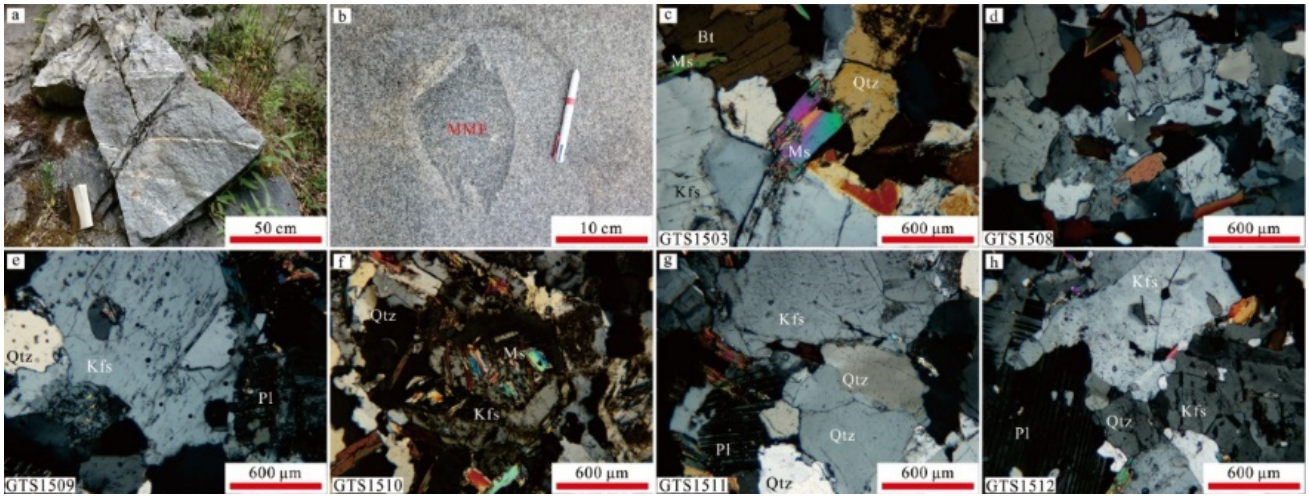

Figure 2. Photographs of representative rocks from the Guangtoushan pluton (in field and under microscope). (**a**,**b**): Field photographs of monzogranite and MME; (**c**) granite; (**d**–**f**) monzogranite; (**g**) granite; (**h**) quartz diorite. *Abbreviations*: MME—mafic microgranular enclave; Qtz—quartz; Ms—muscovite; Bt—biotite; Kfs—K-feldspar; Pl—Plagioclase.

The Miba pluton (Figure 1b), located in south of the late Mesozoic Hui-Cheng basin with an exposure area of >200 km^2, intruded into the Silurian sedimentary sequences

and is mainly composed of monzogranite, granodiorite, and minor quartz diorite [39]. In the present study, six monzogranite or porphyritic monzogranite and two quartz diorite samples were collected from the Miba pluton. Photographs of representative rock samples in field and under microscope are shown in Figure 3. Monzogranite or porphyritic monzogranite have similar mineral assemblage of ~30% plagioclase, ~35% K-feldspar (perthite), ~20% quartz, ~10% amphibole, and ~5% biotite, while quartz diorite consists of ~50% plagioclase, ~15% K-feldspar (perthite), ~15% quartz, ~15% amphibole, and 5% biotite.

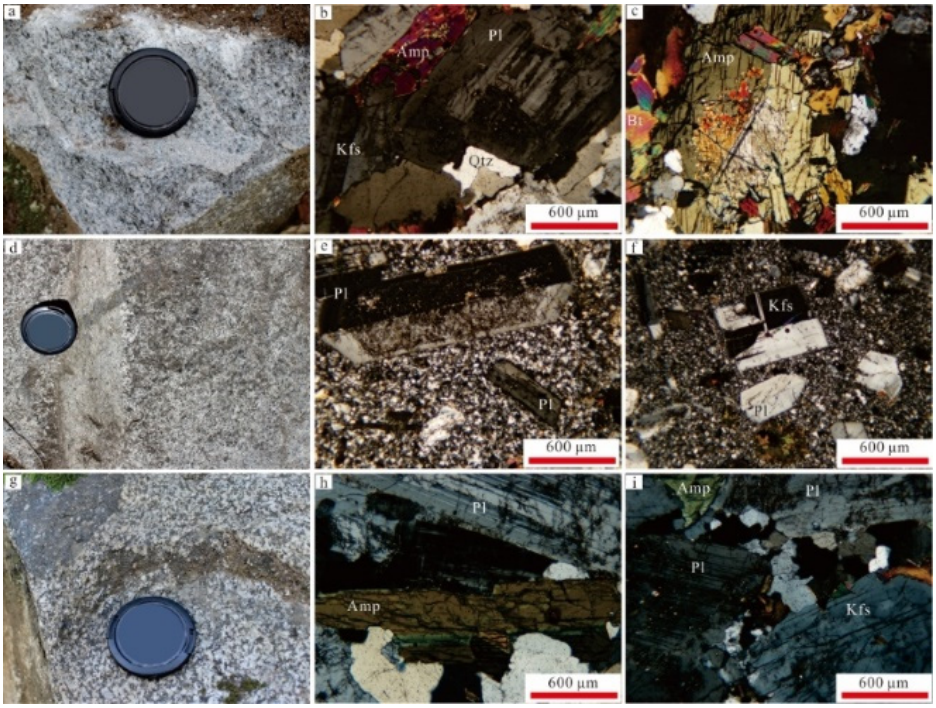

Figure 3. Photographs of representative rocks from the Miba pluton (in field and under microscope); (**a**–**c**): Granodiorite; (**d**–**f**) granodioritic porphyre; (**g**–**i**) quartz diorite. *Abbreviations*: Qtz—quartz; Amp—amphibole; Bt—biotite; Kfs—K-feldspar; Pl—plagioclase.

5. Analytical Results

5.1. Geochemical Composition of Whole Rocks

The analytical results of major and trace elemental contents obtained on thirteen rock samples of the Guangtoushan pluton and eight rock samples of the Miba pluton are given as Supplementary Materials in Table S1.

In the $K_2O + Na_2O$-versus-SiO_2 diagram, the granitic rocks of both plutons are plotted mainly in the fields for granite and granodiorite and minor in the field for diorite (Figure 4), while when plotted in the K_2O-versus-SiO_2 diagram, most of them fall in the fields for calc-alkaline and high-K calc-alkaline rocks (Figure 4). Different rock types of the Guangtoushan pluton have variable contents of major elements and high A/NK and A/CNK values, belonging to the peraluminous series (Figure 4). Monzogranite rocks contain 67.97–71.12 wt.% SiO_2 and 16.46–18.98 wt.% Al_2O_3, and have variant Na_2O/K_2O values of 0.98 to 3.55 and relatively low CaO, $^{T}Fe_2O_3$, and MgO contents. Granite rocks have 72.23–74.77 wt.% SiO_2, 14.58–15.62 wt.% Al_2O_3, and low CaO, $^{T}Fe_2O_3$, and MgO contents. Their A/CNK values are higher than 1.1, also belonging to peraluminous series. Quartz diorites have 62.52–64.82 wt.% SiO_2, 19.08–18.90 wt.% Al_2O_3, and high Na_2O/K_2O values and CaO, $^{T}Fe_2O_3$, and MgO contents. Compared to the Guangtoushan pluton, monzogranite and quartz diorite of the Miba pluton have relatively low SiO_2 and Al_2O_3 as well as high CaO, $^{T}Fe_2O_3$, and MgO contents. A/CNK values of monzogranite are 0.95 to 1.03 and those of quartz diorite are 0.86–0.89, belonging to metaluminous to slightly peraluminous series (Figure 4). Despite granitic rocks from the Guangtoushan pluton yield higher Zr contents than granitic

rocks from the Miba pluton (153–736 ppm and 42.3–166 ppm, respectively), all samples in this study display analogous distribution patterns in the primitive-mantle and chondrite normalization diagrams: all of them have enrichment in light REEs and large-ion lithophile elements (such as Rb, K, and Ba), depletion in high-field-strength elements (Nb, Ta, and Ti), and slightly negative Eu anomaly (Figure 5).

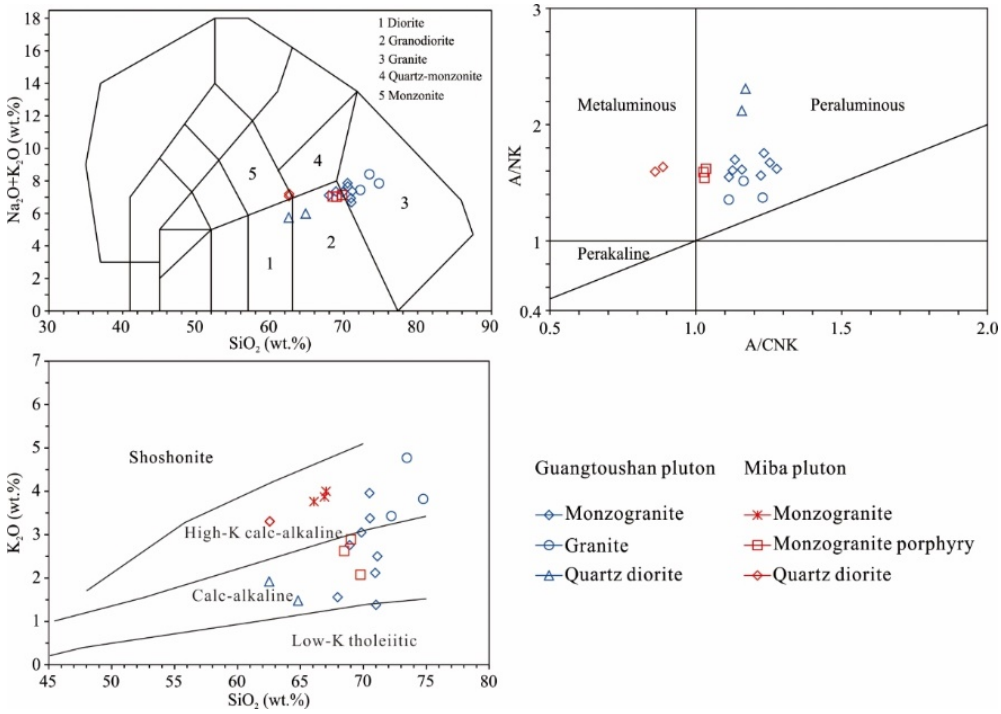

Figure 4. Plots for major elemental compositions of the Guangtoushan and Miba granite plutons exposed in South Qinling [40–42].

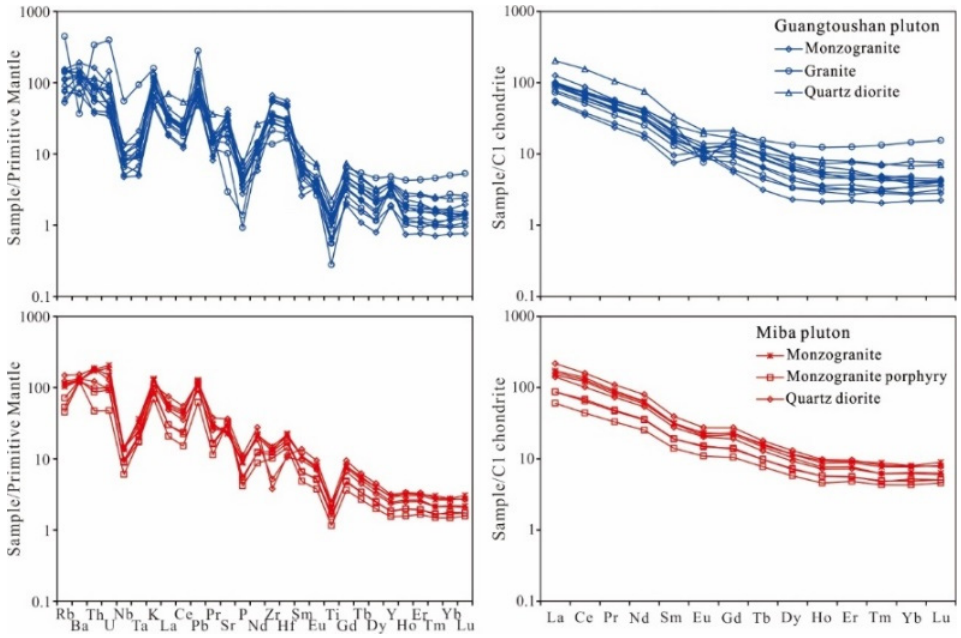

Figure 5. Plots for trace elements and REEs of the Early Mesozoic granite plutons exposed in South Qinling. Data sources: [5,6,27] and this study. Normalization value data are from [43].

5.2. Zircon U-Pb Isotopic Ages

Zircon grains, separated from five samples of the Guangtoushan pluton (samples GTS1502, GTS1503, GTS1506, GTS1507, and GTS1512) and one sample of the Miba pluton (sample CX1717), were analyzed to obtain U-Pb isotopic ages via the LA-ICP-MS technique. The analytical results are given as Supplementary Materials in Table S2. Zircon grains from both plutons are columnar in shape and have grain sizes of ~60 μm to ~300 μm. Most grains have oscillatory zonings shown in the CL images (Figure 6) and U/Th values higher than 0.1, indicating magmatic origin. Only the age data having concordant degrees higher than 90% are used in this study. Zircon U-Pb isotopic data are plotted in the concordia diagrams (Figure 7).

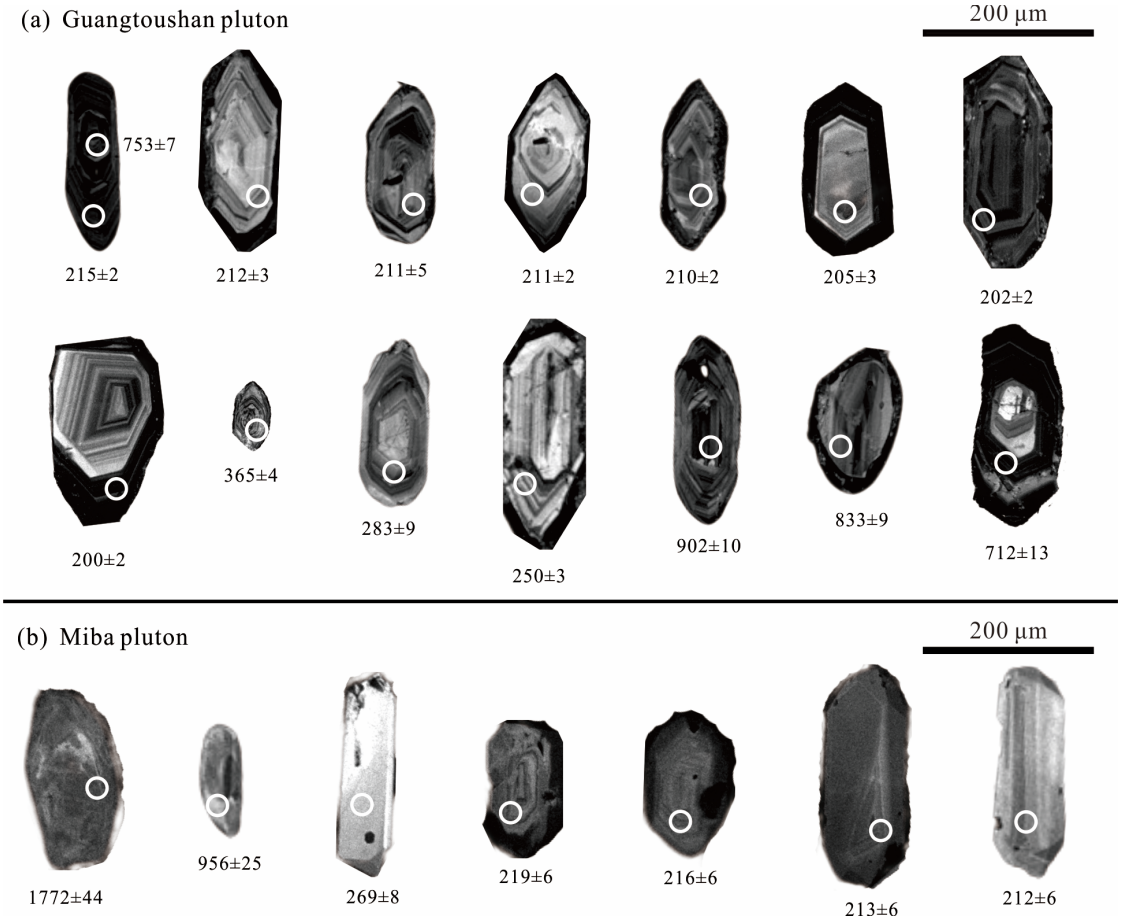

Figure 6. Cathodoluminescence (CL) images of representative zircon grains from the Guangtoushan and Miba plutons.

Guangtoushan pluton: Thirty-one zircon grains from the monzogranite sample GTS1502 gave variable U-Pb isotopic ages. Out of those, twenty-eight analytical spots gave late Triassic U-Pb isotopic ages, with a weighted mean $^{206}Pb/^{238}U$ age value of 205.5 ± 2.2 Ma (n = 20, MSWD = 3.1). The remaining three analytical spots yielded U-Pb isotopic ages ranging from Devonian to Neoproterozoic. These old grains should be inherited zircons originated from the magma source. Nineteen out of twenty zircon grains from monzogranite sample GTS1507 gave late Triassic U-Pb isotopic ages, with a weighted mean $^{206}Pb/^{238}U$ age value of 208.6 ±1.9 Ma (n = 18, MSWD = 1.6). The final one had a Neoproterozoic age. Twenty-six zircon grains from granite sample GTS1503 mostly yielded late Triassic U-Pb isotopic ages, with a weighted mean $^{206}Pb/^{238}U$ age value of 202.2 ± 1.3 Ma (n = 19, MSWD = 1.6). Only one grain gave an early Carboniferous age. Nine out of sixteen zircon grains gave late Triassic U-Pb isotopic ages, with a weighted mean $^{206}Pb/^{238}U$ age value

of 214.9 ± 1.8 Ma (n = 9, MSWD = 1.0). The remaining seven spots had variable ages of Early Triassic, Devonian, Neoproterozoic, and Mesoproterozoic, indicating complex crustal components in the magma source. Twenty-eight zircon grains from quartz diorite sample GTS1512 were analyzed. Eighteen ones among them yielded late Triassic U-Pb isotopic ages, with a weighted mean $^{206}Pb/^{238}U$ age value of 212.0 ± 1.2 Ma (n = 15, MSWD = 0.9). The remaining ten grains had age values ranging from Neoproterozoic to Early Triassic.

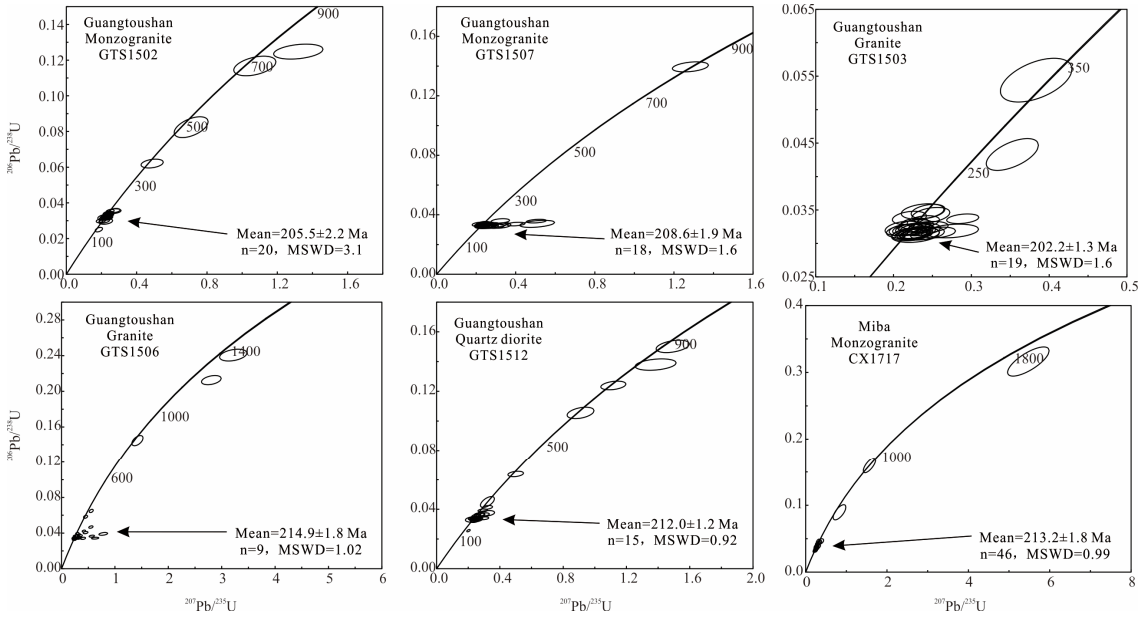

Figure 7. Concordia diagrams of zircon U-Pb isotopic data for the Guangtoushan and Miba plutons.

Miba pluton: Fifty-seven zircon grains from monzogranite sample CX1717 yielded variable U-Pb isotopic ages. Among them, forty-six analytical spots gave Early Mesozoic U-Pb isotopic ages, with a weighted mean $^{206}Pb/^{238}U$ age value of 213.2 ± 1.8 Ma (n = 46, MSWD = 1.0). The remaining grains obviously had old U-Pb isotopic ages, the majority being of Permian to Early Triassic and the minority of Neoproterozoic and Paleoproterozoic, implying that they are inherited zircon grains from the magma source.

5.3. Sr-Nd-Pb Isotopic Compositions of Whole Rocks

Analytical results of Sr-Nd-Pb isotopic compositions of twenty-one rock samples from the Guangtoushan and Miba plutons are given as Supplementary Materials in Table S3. Initial isotopic values were calculated back to 210 Ma. Generally, three rock types of the Guangtoushan pluton have variable Rb/Sr and Sm/Nd values, resulting in a discrepancy in the initial Sr and Nd isotopic compositions (Figure 8). Their initial $^{87}Sr/^{86}Sr$ values range from 0.7050 to 0.7091, initial ε_{Nd} values range from −4.5 to −12.9, and depleted-mantle Nd model ages (T_{DM2}) range from 1.36 Ga to 2.04 Ga. Compared to the Guangtoushan pluton, the rock samples of the Miba pluton exhibit relatively constant and depleted Sr and Nd isotopic compositions, having initial $^{87}Sr/^{86}Sr$ values of 0.7060 to 0.7085 and initial ε_{Nd} values of −5.4 to −9.5 (Figure 8). Remarkably, rocks from the Guangtoushan pluton have low initial Pb isotopic values ($^{206}Pb/^{204}Pb$ from 16.29 to 17.68, $^{207}Pb/^{204}Pb$ from 15.43 to 15.53, and $^{208}Pb/^{204}Pb$ from 37.88 to 38.89), while those from the Miba pluton are enriched in Pb isotopic composition, distinguishable from the Guangtoushan, Dongjiangkou, and Baoji plutons exposed in South and North Qinling (Figure 9). They have high initial $^{206}Pb/^{204}Pb$ values from 18.19 to 18.63 and initial $^{208}Pb/^{204}Pb$ values from 38.77 to 39.17, implying high U/Pb and Th/Pb in the magma source.

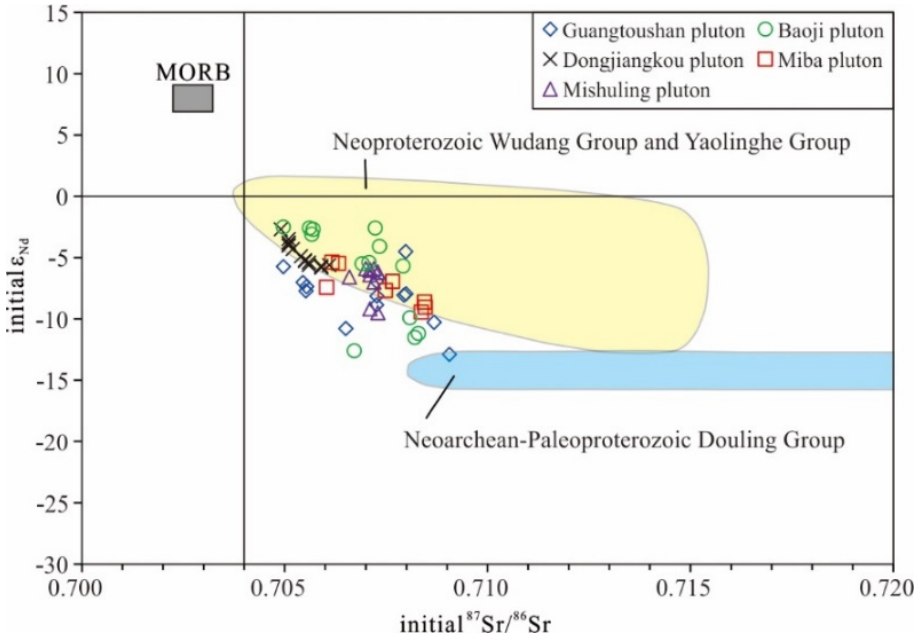

Figure 8. Plot for Sr-Nd isotopic compositions of the Early Mesozoic granite plutons exposed in South Qinling. Data sources: [5,6,27] and this study.

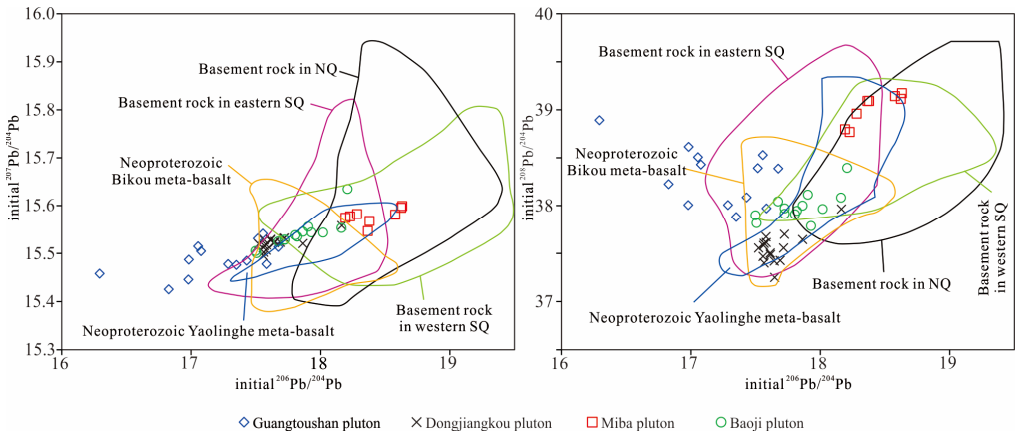

Figure 9. Plots for Pb isotopic composition of the Early Mesozoic granite plutons exposed in South Qinling. Data sources: [6,27] and this study.

6. Discussion

6.1. Geochemical Characteristics of Magma Sources

The analytical results of zircon U-Pb isotopic dating in the present study confirm that the Guangtoushan and Miba plutons were formed coevally in Late Triassic after the collision of the South and North China blocks [12]. Granitic rocks from these plutons display substantial variances in Sr-Nd-Pb isotopic features (Figures 8 and 9), most likely suggesting compositional diversities of the magma sources. As is well known, inherited zircon grains in magmatic rocks could be an efficient indicator for tracing source components from which the magma was derived [44]. The Miba pluton contains a small amount of inherited zircon grains formed from the Permian to Early Triassic period, and rarely in the Precambrian age (Figure 10). Granitic rocks of the Guangtoushan pluton incorporate the complex component of inherited zircon, as revealed in the distribution pattern of U-Pb isotopic ages (Figure 10), distinct from the coeval granitoid plutons in South Qinling, such as the Miba, Baoji, and Mishuling plutons, but similar to the Dongjiangkou pluton. The inherited zircon grains in the Guangtoushan pluton crystallized mostly in the Neoproterozoic and late Paleozoic to

Early Triassic period, with a minority in the Early Proterozoic age, implying compositional complexity of the magma sources. Such zircon grains can be found in both igneous and sedimentary rocks in South Qinling.

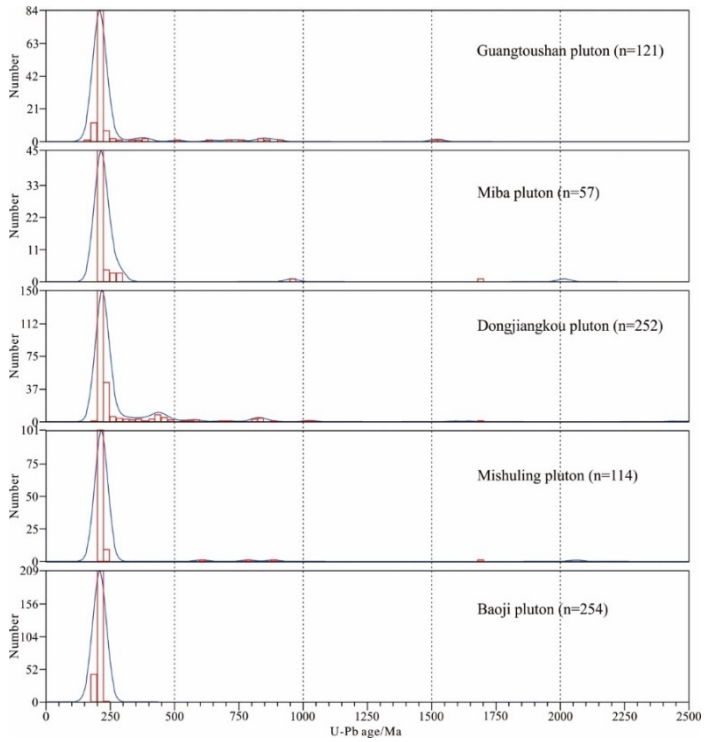

Figure 10. Distribution of zircon U-Pb isotopic ages of Early Mesozoic granite plutons exposed in South Qinling, showing differences in component of inherited zircon grains. Data sources: [5,6,27] and this study.

Most rocks of the Guangtoushan and Miba plutons exhibit compositional similarity in elemental geochemistry (Figure 4), but rocks of the former are characterized by more variance in major elemental contents and initial values of Sr-Nd-Pb isotopes (Figures 4, 8 and 9). In general, they have higher SiO_2 and Al_2O_3 contents, but lower K_2O, CaO, and MgO contents (Figure 4). They yield high Zr contents and A/CNK values and belong to strongly peraluminous series. Some of them noticeably contain aluminous-rich minerals, such as muscovite, a kind of diagnostic mineral of S-type granite, and are likely of S-type granite. In combination of these characteristics of geochemical composition and inherited zircon, meta-sedimentary rocks beneath South Qinling must have substantially contributed to the magma sources. This is coincident with the observations previously reported in the literature [26,32], which showed that the Guangtoushan pluton displays petrologic features of S-type granite with relatively low melting temperatures and then proposed a mixture of greywacke and argillaceous rock as the potential source for the magma(s).

Compared to the Guangtoushan pluton, rocks of the Miba pluton are relatively homogeneous in geochemical compositions of elements and Sr-Nd-Pb isotopes and have lower SiO_2 and Al_2O_3 contents, but higher CaO, MgO, Cr, and Ni contents. They yield low Zr contents and A/CNK values of 0.86–1.03, indicating that the samples from the Miba pluton belong to metaluminous to weakly peraluminous series. Amphibole can be commonly found in most of the rocks, a kind of diagnostic mineral of I-type granite, while muscovite, commonly found in S-type granite, is absent in petrological observations (Figure 3). These features imply that this pluton is I-type granite and the magma source was composed mainly of meta-igneous rocks. A similar deduction was recently proposed that the Miba pluton was produced from dehydration melting of igneous rocks (likely meta-basalt) in South Qinling [45].

6.2. Origin of the Early Mesozoic Granitoid Plutons

The South Qinling terrain records intensive magmatism of the Early Mesozoic in the late orogenic stages, resulting in a wide distribution of numerous large granitoid plutons in this terrain. They are characterized by complex rock types, various emplacement ages, and various compositions, demonstrating diversity in magma sources and probably in tectonic settings. For instance, the Hejiazhuang pluton in the western part of South Qinling, being one of the earlier forming plutons and emplaced at ~248 Ma, has relatively high Na_2O, Sr, Cr, and Ni contents and $Mg^{\#}$ values, low Y and Yb contents, and is depleted in Nb, Ta, P, and Ti elemental and Hf isotopic composition. These geochemical features were proposed as evidence for an origin of partial melting of the subducted oceanic crust and sedimentary material in an arc setting [31,46]. The Wulong and Dongjiangkou plutons in the east of the Hui-Cheng basin are composed of dioritic and granitic rocks forming at ~220–210 Ma and have been interpreted as magmatic products in the post-collisional setting [6,22]. The ~242 Ma Xihe and ~214 Ma Baijiazhuang plutons exposed in the west of the basin, mainly consisting of peraluminous granite, yield S-type affinity in geochemical composition and mineral assemblage and were interpreted to be derived from pelitic source [4].

Granitic rocks in the Dongjiangkou and Wulong plutons, having adakitic affinity in geochemical composition and often containing mafic microgranular enclaves, were proposed as the mixing or mingling products of mafic and felsic magmas [6,22]. Similarly, granites of the Guangtoushan and Miba plutons partly display adakitic feature in geochemistry and occasionally contain mafic microgranular enclaves. The Guangtoushan pluton has variable Nd isotopic composition (Figure 8), implying the input of mafic magma in different degrees. Considering the combination of mineral assemblages, geochemical features, and the occurrence of inherited zircon, felsic magma(s) of this pluton should be derived from such a source mainly of meta-sedimentary rocks beneath the South Qinling terrain. The partial melting was induced by heating of the up-welling asthenosphere in a post-collision setting [6]. Akin to the Mishuling pluton [5], the Miba pluton originated mainly from partial melting of meta-igneous rocks, lead to relatively homogeneous in geochemical compositions of elements and Sr-Nd-Pb isotopes. In conclusion, the compositional diversity, recorded in the Guangtoushan and Miba as well as other Early Mesozoic granitoid plutons in the Qinling orogenic belt, was the result of the heterogeneous crust underneath the orogenic belt and was partly controlled by the magma mixing or mingling process.

7. Conclusions

Granitic rocks of the Guangtoushan pluton, formed at about 215 Ma to 202 Ma, are characterized by compositional diversity and part of them have geochemical affinity of S-type granite. They display large variances in Sr-Nd isotopic composition, with initial $^{87}Sr/^{86}Sr$ values of 0.7050–0.7091 and initial ε_{Nd} values of −4.5 to −12.9, and are relatively low in initial Pb isotopic compositions. The rocks partly contain numerous inherited zircon grains of different crystallization ages. These geochemical appearances point to complex source components of the magmas, most likely mixtures of ancient sedimentary and igneous rocks underneath the South Qinling orogenic belt.

The Miba pluton, having geochemical feature of I-type granite, was emplaced at ~213 Ma and is consistent and relatively depleted in Sr-Nd isotopic composition, with initial $^{87}Sr/^{86}Sr$ values of 0.7060–0.7085 and initial ε_{Nd} values of −5.4 to −9.5. All the rocks are portrayed by high initial Pb isotopic compositions. These geochemical characteristics imply igneous rocks deeply seated in the South Qinling basement as the major source of the magmas.

The compositional diversity recorded in Early Mesozoic granitoid plutons in the Qinling orogenic belt indicates that the crust underneath the orogenic belt is heterogeneous.

Supplementary Materials: The following supporting information can be downloaded at: https://www.mdpi.com/article/10.3390/geosciences14050138/s1, Table S1: Contents of major and trace elements of the Guangtoushan and Miba plutons; Table S2: Zircon U-Pb isotopic ages of the Guangtoushan and Miba plutons obtained by the LA-ICP-MS technique; Table S3: Sr-Nd-Pb isotopic compositions of the Guangtoushan and Miba plutons.

Author Contributions: Writing—original draft, R.Y. and X.H.; Writing- editing and review, J.H. and F.C.; Field survey and data interpretation, R.Y., X.H., D.H. and J.Z.; Lab analyses, R.Y. and W.L.; Illustrations, R.Y., J.Z. and J.H. All authors have read and agreed to the published version of the manuscript.

Funding: This study was financially supported by the National Key Research and Development Plan of China (grant No. 2023YFC2908600) and the National Natural Science Foundation of China (grant Nos. 42202069 and 41872049).

Data Availability Statement: All data reported in the paper are given as Supplementary Materials in Table S1, Table S2, and Table S3.

Acknowledgments: The authors thank Zhenhui Hou and Ping Xiao for assistance with the analysis, He Zhang for help during the field work, and two anonymous reviewers for their constructive comments and suggestions to improve the manuscript.

Conflicts of Interest: The authors here declare that they have no known competing financial interests or personal relationship that could have appeared to influence the work reported in this paper.

References

1. Patiño Douce, A.E.; Beard, J.S. Dehydration-melting of biotite gneiss and quartz amphibolite from 3 to 15 kbar. *J. Petrol.* **1995**, *36*, 707–738. [CrossRef]
2. Patiño Douce, A.E. Effects of pressure and H_2O content on the compositions of primary crustal melts. *Earth Environ. Sci. Trans. R. Soc. Edinb.* **1996**, *87*, 11–21.
3. Altherr, R.; Holl, A.; Hegner, E.; Langer, C.; Kreuzer, H. High-potassium, calc-alkaline I-type plutonism in the European Variscides: Northern Vosges (France) and northern Schwarzwald (Germany). *Lithos* **2000**, *50*, 51–73. [CrossRef]
4. Dou, J.-Z.; Siebel, W.; He, J.-F.; Chen, F. Different melting conditions and petrogenesis of peraluminous granites in western Qinling, China, and tectonic implications. *Lithos* **2019**, *336–337*, 97–111. [CrossRef]
5. Dou, J.-Z.; Huang, X.-G.; Chen, F. Successive magma mixing in deep-seated magma chambers recorded in zircon from mafic microgranular enclaves in the Triassic Mishuling granitic pluton, Western Qinling, Central China. *J. Asian Earth Sci.* **2021**, *207*, 104656. [CrossRef]
6. He, J.; Fan, X.; Zhao, J.-X.; Huo, D.-Y.; Zhang, N.-Z.; Chen, F. Petrogenesis of the Triassic Dongjiangkou pluton in the South Qinling orogenic belt, Central China: Insufficient magma mixing of mafic and felsic magmas. *Lithos* **2023**, *456–457*, 107312. [CrossRef]
7. Meng, Q.-R.; Zhang, G.-W. Timing of collision of the North and South China blocks: Controversy and reconciliation. *Geology* **1999**, *27*, 123–126. [CrossRef]
8. Meng, Q.-R.; Zhang, G.-W. Geologic framework and tectonic evolution of the Qinling orogen, Central China. *Tectonophysics* **2000**, *323*, 183–196. [CrossRef]
9. Dong, Y.-P.; Zhang, G.-W.; Neubauer, F.; Liu, X.-M.; Genser, J.; Houzenberger, C. Tectonic evolution of the Qinling orogen, China: Review and synthesis. *J. Asian Earth Sci.* **2011**, *41*, 213–237. [CrossRef]
10. Ratschbacher, L.; Hacker, B.R.; Calvert, A.; Webb, L.E.; Grimmer, J.C.; McWilliams, M.O.; Ireland, T.; Dong, S.; Hu, J. Tectonics of the Qinling (Central China): Tectonostratigraphy, geochronology, and deformation history. *Tectonophysics* **2003**, *336*, 1–53. [CrossRef]
11. Dong, Y.-P.; Liu, X.-M.; Neubauer, F.; Zhang, G.-W.; Tao, N.; Zhang, Y.; Zhang, X.; Li, W. Timing of Paleozoic amalgamation between the North China and South China Blocks: Evidence from detrital zircon U-Pb ages. *Tectonophysics* **2013**, *586*, 173–191. [CrossRef]
12. Dong, Y.P.; Santosh, M. Tectonic architecture and multiple orogeny of the Qinling Orogenic Belt, Central China. *Gondwana Res.* **2016**, *29*, 1–40. [CrossRef]
13. Hu, J.; Liu, X.; Chen, L.; Qu, W.; Li, H.; Geng, J. A ~2.5 Ga magmatic event at the northern margin of the Yangtze craton: Evidence from U-Pb dating and Hf isotope analysis of zircons from the Douling Complex in the South Qinling orogen. *Chin. Sci. Bull.* **2013**, *58*, 3564–3579. [CrossRef]
14. Nie, H.; Yao, J.; Wan, X.; Zhu, X.-Y.; Siebel, W.; Chen, F. Precambrian tectonothermal evolution of South Qinling and its affinity to the Yangtze Block: Evidence from zircon ages and Hf-Nd isotopic compositions of basement rocks. *Precambrian Res.* **2016**, *286*, 167–179. [CrossRef]

15. Hui, B.; Dong, Y.-P.; Cheng, C.; Long, X.-P.; Liu, X.-M.; Yang, Z.; Sun, S.-S.; Zhang, F.-F.; Varga, J. Zircon U-Pb chronology, Hf isotope analysis and whole-rock geochemistry for the Neoarchean-Paleoproterozoic Yudongzi complex, northwestern margin of the Yangtze craton, China. *Precambrian Res.* **2017**, *301*, 65–85. [CrossRef]
16. Hu, F.; Liu, S.; Santosh, M.; Deng, Z.; Wang, W.; Zhang, W.; Yan, M. Chronology and tectonic implications of Neoproterozoic blocks in the South Qinling Orogenic Belt, Central China. *Gondwana Res.* **2016**, *30*, 24–47. [CrossRef]
17. Zhao, L.; Li, Y.; Rong, C.; Li, F.; Xiang, H.; Zheng, J.; Brouwer, F.M. Geochemical and zircon U-Pb-Hf isotopic study of volcanic rocks from the Yaolinghe Group, South Qinling orogenic belt, China: Constraints on the assembly and breakup of Rodinia. *Precambrian Res.* **2022**, *371*, 106603. [CrossRef]
18. Li, Q.-W.; Zhao, J.-H. Petrogenesis of the Wudang mafic dikes: Implications of changing tectonic settings in South China during the Neoproterozoic. *Precambrian Res.* **2016**, *272*, 101–114. [CrossRef]
19. Nie, H.; Wan, X.; Zhang, H.; He, J.-F.; Hou, Z.-H.; Siebel, W.; Chen, F. Ordovician and Triassic mafic dykes in the Wudang terrene: Evidence for opening and closure of the South Qinling ocean basin, central China. *Lithos* **2016**, *266–267*, 1–15. [CrossRef]
20. Qin, J.-F.; Lai, S.-C.; Grapes, R.; Diwu, C.-R.; Ju, Y.-J.; Li, Y.-F. Geochemical evidence for origin of magma mixing for the Triassic monzonitic granite and its enclaves at Mishuling in the Qinling orogen (central China). *Lithos* **2009**, *112*, 259–276. [CrossRef]
21. Qin, J.-F.; Lai, S.-C.; Diwu, C.-R.; Ju, Y.-J.; Li, Y.-F. Magma mixing origin for the post-collisional adakitic monzogranite of the Triassic Yangba pluton, Northwestern margin of the South China block: Geochemistry, Sr-Nd isotopic, zircon U-Pb dating and Hf isotopic evidences. *Contrib. Mineral. Petrol.* **2010**, *159*, 389–409. [CrossRef]
22. Qin, J.-F.; Lai, S.-C.; Li, Y.-F. Multi-stage granitic magmatism during exhumation of subducted continental lithosphere: Evidence from the Wulong pluton, South Qinling. *Gondwana Res.* **2013**, *24*, 1108–1126. [CrossRef]
23. Wang, X.-X.; Wang, T.; Castro, A.; Pedreira, R.; Lu, X.-X.; Xiao, Q.-H. Triassic granitoids of the Qinling orogen, central China: Genetic relationship of enclaves and rapakivi-textured rocks. *Lithos* **2011**, *126*, 369–387. [CrossRef]
24. Wang, X.-X.; Wang, T.; Zhang, C.-L. Neoproterozoic, Paleozoic, and Mesozoic granitoid magmatism in the Qinling Orogen, China: Constraints on orogenic process. *J. Asian Earth Sci.* **2013**, *72*, 129–151. [CrossRef]
25. Dong, Y.-P.; Liu, X.-M.; Zhang, G.-W.; Chen, Q.; Zhang, X.; Li, W.; Yang, C. Triassic diorites and granitoids in the Foping area: Constraints on the conversion from subduction to collision in the Qinling orogen, Central China. *J. Asian Earth Sci.* **2012**, *47*, 123–142. [CrossRef]
26. Lu, Y.-H.; Zhao, Z.-F.; Zheng, Y.-F. Geochemical constraints on the source nature and melting conditions of Triassic granites from South Qinling in central China. *Lithos* **2016**, *264*, 141–157. [CrossRef]
27. Xue, Y.-Y.; Siebel, W.; He, J.-F.; Zhang, H.; Chen, F. Granitoid petrogenesis and tectonic implications of the Late Triassic Baoji pluton, North Qinling Orogen, China: Zircon U-Pb ages and geochemical and Sr-Nd-Pb-Hf isotopic compositions. *J. Geol.* **2018**, *126*, 119–139. [CrossRef]
28. Li, N.; Chen, Y.-J.; Santosh, M.; Pirajno, F. Compositional polarity of Triassic granitoids in the Qinling Orogen, China: Implication for termination of the northernmost paleo-Tethys. *Gondwana Res.* **2015**, *27*, 244–257. [CrossRef]
29. Jiang, Y.-H.; Jin, G.-D.; Liao, S.-Y. Geochemical and Sr-Nd-Hf isotopic constraints on the origin of Late Triassic granitoids from the Qinling orogen, central China: Implications for a continental arc to continent- continent collision. *Lithos* **2010**, *117*, 183–197. [CrossRef]
30. Jiang, Y.-H.; Jin, G.-D.; Liao, S.-Y.; Zhou, Q.; Zhao, P. Petrogenesis and tectonic implications of ultrapotassic microgranitoid enclaves in late Triassic arc granitoids, Qinling orogen, Central China. *Int. Geol. Rev.* **2012**, *54*, 208–226. [CrossRef]
31. Zhang, C.-L.; Wang, T.; Wang, X.-X. Origin and tectonic setting of the Early Mesozoic granitoids in Qinling Orogenic belt. *Geol. J. China Univ.* **2008**, *14*, 304–316, (In Chinese with English abstract).
32. Deng, Z.-B.; Liu, S.-W.; Zhang, W.-Y.; Hu, F.-Y.; Li, Q.-G. Petrogenesis of the Guangtoushan granitoid suite, central China: Implications for Early Mesozoic geodynamic evolution of the Qinling Orogenic Belt. *Gondwana Res.* **2016**, *30*, 112–131. [CrossRef]
33. Hou, Z.-H.; Wang, C.-X. Determination of 35 trace elements in geological samples by inductively coupled plasma mass spectrometry. *J. Univ. Sci. Technol. China* **2007**, *37*, 940–944. (In Chinese with English abstract)
34. Liu, Y.-S.; Hu, Z.; Gao, S.; Günther, D.; Xu, J.; Gao, C.; Chen, H. In situ analysis of major and trace elements of anhydrous minerals by LA-ICP-MS without applying an internal standard. *Chem. Geol.* **2008**, *257*, 34–43. [CrossRef]
35. Ludwig, K.R. Isoplot3.70 A Geochronological Toolkit for Microsoft Excel. *Berkeley Geochronol. Center Spec. Publ.* **2009**, *4*, 1–76.
36. Chen, F.; Li, X.-H.; Wang, X.-L.; Li, Q.-L.; Siebel, W. Zircon age and Nd-Hf isotopic composition of the Yunnan Tethyan belt, southwestern China. *Int. J. Earth Sci.* **2007**, *96*, 1179–1194. [CrossRef]
37. Liu, S.-W.; Li, Q.-G.; Tian, W.; Wang, Z.-Q.; Yang, P.-T.; Wang, W.; Bai, X.; Guo, R.-R. Petrogenesis of Indosinian Granitoids in Middle-Segment of South Qinling Tectonic Belt: Constraints from Sr-Nd Isotopic Systematics. *Acta Geol. Sin. (Engl. Ed.)* **2011**, *85*, 610–628. [CrossRef]
38. Qin, J.-F.; Lai, S.-C.; Wang, J.; Li, Y.-F. High-Mg adakitic tonalite from the Xichahe area, South Qinling orogenic belt (Central China): Petrogenesis and geological implications. *Int. Geol. Rev.* **2007**, *49*, 1145–1158. [CrossRef]
39. Mu, K.-B. Genesis of Indosinian Intermediate to Felsic Magmatic Rocks in the Mian-Lue Area of the South Qinling Belt and Tectonic Evolution. Master's Thesis, Chang'an University, Chang'an, China, 2020; 111p. (in Chinese with English abstract)
40. Middlemost, E.A.K. Naming materials in the magma/igneous rock system. *Earth-Sci. Rev.* **1994**, *37*, 215–224. [CrossRef]
41. Maniar, P.-D.; Piccoli, P.-M. Tectonic discrimination of granitoids. *Geol. Soc. Am. Bull.* **1989**, *101*, 635–643. [CrossRef]

42. Rickwood, P.-C. Boundary lines within petrologic diagrams which use oxides of major and minor elements. *Lithos* **1989**, *22*, 247–263. [CrossRef]
43. Sun, S.-S.; Mcdonough, W.-F. Chemical and isotopic systematics of oceanic basalts: Implications for mantle composition and processes. *Geol. Soc. London Spec. Publ.* **1989**, *42*, 313–345. [CrossRef]
44. Williams, I.S. Response of detrital zircon and monazite, and their U–Pb isotopic systems, to regional metamorphism and host-rock partial melting, Cooma Complex, southeastern Australia. *Aust. J. Earth Sci.* **2001**, *48*, 557–580. [CrossRef]
45. Han, B.-N.; Jiang, Y.-H.; Liu, Y.-C.; Ni, C.-Y. Middle to Late Triassic felsic and mafc magmatism in the eastern West Qinling Orogen, Central China: A record of the Paleo-Tethyan oceanic crust advance to retreat. *Lithos* **2024**, *464–465*, 107451. [CrossRef]
46. Yang, P.-T.; Liu, S.-W.; Li, Q.-G.; Wang, Z.-Q.; Zhang, F.; Wang, W. Chronology and petrogenesis of the Hejiazhuang granitoid pluton and its constraints on the early Triassic tectonic evolution of the South Qinling Belt. *Sci. China (Ser. D Earth Sci.)* **2014**, *57*, 232–246. [CrossRef]